Trans Indian Inst Met (2022) 75(8):2031–2039
https://doi.org/10.1007/s12666-022-02572-y

ORIGINAL ARTICLE

Effect of Lanthanum and Cerium on Inclusions in GCr15 Bearing Steel

Xiang-yu Wu[1] · Bei-bei Liu[1] · Qian-ren Tian[1] · Jian-bo Xie[1] · Jian-xun Fu[1]

Received: 8 December 2021 / Accepted: 22 February 2022 / Published online: 1 April 2022

Abstract To investigate the effect of La-Ce on inclusions in GCr15 bearing steel and its modification mechanism, relevant industrial tests were carried out. The results show that the typical inclusions in GCr15 bearing steel were long strip MnS and irregular Al_2O_3. At 1600 °C, with increasing La-Ce content, the transformation sequence of inclusions was $Al_2O_3 \rightarrow REAlO_3 \rightarrow RE_2O_3 \rightarrow RE_2O_2S \rightarrow RE_2O_2S + RE_xS_y$ (RE was La-Ce). The formation of RE_xS_y and RE_2O_2S was the fundamental reason for reduction in the quantity and size of MnS, and the spheroidization of inclusions was caused by $REAlO_3$ and RE_2O_3 formed by La-Ce replacing Al in Al_2O_3. Considering the production cost and modification effect, the addition amount of La-Ce in the steel must reach at least 90 ppm to effectively improve the morphologies of all the inclusions thermodynamically, and the content of S could be remarkably reduced when the addition amount reached 120 ppm.

Keywords La-Ce · Inclusions · GCr15

1 Introduction

GCr15 bearing steel is one of the strictest requirements in the special steels, because of its good wear resistance, high fatigue life, so it is widely used to manufacture all kinds of industrial bearing equipment [1, 2]. Due to the tough and complex service environment of GCr15 bearing steel, it is necessary to maintain good performance under high temperature and pressure for a long time. In such extreme working environment, inclusions will have a particularly significant impact on performance [3–6], so the overall control requirements are more stringent. Traditionally, the main methods used for modification of the inclusions are additions of Mg [7], Ca [8] to liquid steel. Although these studies have made some progresses in reducing the number of inclusions and controlling the morphology of inclusions, the results mainly focus on the control of oxide inclusions, and the overall improvement effect of sulfide is not satisfactory. Recently, rare earth elements have been added to steel for modifying the inclusions, with good effects on both oxide inclusions and sulfide inclusions.

La and Ce elements, with the highest reserves in rare earth, have active chemical properties, strong binding ability with O and S, and can regulate the morphology of inclusions [9–12]. So far, some scholars have studied the modification of inclusions by adding La and Ce elements to steel. Li et al. [13]. studied the effect of Ce on low-carbon medium manganese steel, indicating that Ce could remarkably reduce oxygen content and directly modify Al_2O_3 to Ce_2O_2S, and the amount of rare earth inclusions increased with increasing rare earth content, but the size of inclusions first decreased and then increased. Gong et al. [14] analyzed the effect of La on S, P, As elements in low alloy steel, showing that La could first form La_2O_2S, then form La_2S_3 and La_2O_2S wrapped by La_2S_3. In the subsequent solidification process, due to the high activity of La, P and As would converge on the $La_2O_2S \cdot La_2S_3$ to form complex inclusions. Ren et al. [15] discussed the effect of Ce on inclusions in ultra-low carbon Al-Killed steel, concluding that the mass ratio of Ce and O determined the type of inclusions in steel; the type of inclusions were $Al_2O_3 + CeAlO_3$ as Ce/O was 0–2.92, the inclusions were

✉ Jian-xun Fu
fujianxun@shu.edu.cn

[1] Center for Advanced Solidification Technology (CAST), School of Materials Science and Engineering, Shanghai University, Shanghai 201900, China

$CeAlO_3 + Ce_2O_2S$ as Ce/O was 2.92 to 8.75, when Ce/O was ≥ 8.75, inclusions were $Ce_2O_2S + CeS$.

However, there are few studies on the effects of La and Ce on inclusions in high cleanliness GCr15 bearing steel, mainly concentrated on the laboratory research. In addition, different from the large-scale addition amount in the laboratory, the addition process and amount of La and Ce must be formulated from various factors such as cost and smooth operation of smelting process in actual industrial production. Based on this, the industrial tests of La-Ce composite treated GCr15 bearing steel were carried out in this work, and the modification effect and mechanism of La-Ce on inclusions were deeply analyzed under different addition amounts.

2 Methods

The industrial tests of La and Ce composite treated GCr15 bearing steel were carried out in a steel plant. The production process of GCr15 bearing steel is LD-LF-RH-CC. To avoid the direct reaction between rare earth and oxygen in liquid steel, La-Ce rare earth alloy was added to the ladle at the end of LF refining when T[O] content was 9 ∼ 10 ppm. In the subsequent RH refining process, the circulating liquid steel can not only promote the full reaction between rare earth and inclusions to improve the modification effect, but also can make the formed rare earth inclusions distributed more evenly. In these industrial tests, La and Ce rare earth alloys with mass ratio of 1:2 were used, and the designed addition amount was 50, 100 and 150 ppm, respectively.

Four industrial test details were given here. Where, furnace A was the contrast group without rare earth addition, and 50, 100, 150 ppm La-Ce rare earth were added to the furnaces B, C, D. The chemical compositions of four experimental steels after element tests are shown in Table 1. La-Ce reduced the S content, but had little effect on T[O], indicating that La-Ce had no obvious removal effect on oxidized inclusions. The content of rare earth is low in steel. The main reasons are that: (1) the yield of rare earth itself is low; (2) the formed rare earth inclusions circulate with the liquid steel in the RH refining process, resulting in part of them floating up and further being adsorbed by the slag layer under the action of argon blowing and stirring.

In industrial tests, different La-Ce content treated GCr15 bearing steels were processed into rolled steels with a diameter of 80 mm. To analyze it more comprehensively, samples were taken out at the edge, quarter and center of rolled steels, respectively, as shown in Fig. 1.

3 Results and Discussion

3.1 Effect of La-Ce on Inclusions in GCr15 Bearing Steel

3.1.1 Effect of La-Ce on the Quantity and Size of Inclusions

The optical morphology and distribution of inclusions at various positions in the rolled steels with different La-Ce additions at 100 × magnification, as shown in Fig. 2. When La-Ce was not added, there were some long strip inclusions in steel, and the distribution of inclusions was more concentrated. With the increase in La-Ce addition, the aspect ratio of long strip inclusions began to decrease, and the distribution of inclusions was changed from chain to disperse. As the addition of La-Ce reached 150 ppm, nearly all the long strip inclusions disappeared; finally, all inclusions became more distributed.

To conduct more detailed quantitative analysis, metallographic photographs at 200 × magnification at different positions of samples were randomly selected, and the density and average equivalent diameter of inclusions were calculated and counted by the Image-Pro Plus software, as shown in Fig. 3.

Figure 3a shows that La-Ce had a certain removal effect on inclusions in steel; with the increase in addition, the density of inclusions decreased from 51 to 40/mm^2. Besides, when La-Ce was not added, the number fluctuation of inclusions in steel was great from edge to center, but with increasing La-Ce addition to steel, the number fluctuation of inclusions became smaller and smaller. At 150 ppm addition, the distribution of inclusions in steel

Table 1 The chemical compositions of four experimental GCr15 bearing steels after element tests (mass %)

Furnace	C	Si	Mn	P	S	Cr	As	T[O]	Al	La	Ce
A	1.0	0.24	0.34	0.013	0.0021	1.48	0.003	0.0007	0.021	/	/
B	0.99	0.25	0.34	0.013	0.0020	1.49	0.003	0.0007	0.020	< 0.0015	< 0.0015
C	1.0	0.23	0.34	0.014	0.0018	1.48	0.003	0.0007	0.020	< 0.0015	< 0.0015
D	0.99	0.24	0.33	0.012	0.0017	1.50	0.003	0.0007	0.020	< 0.0015	< 0.0015

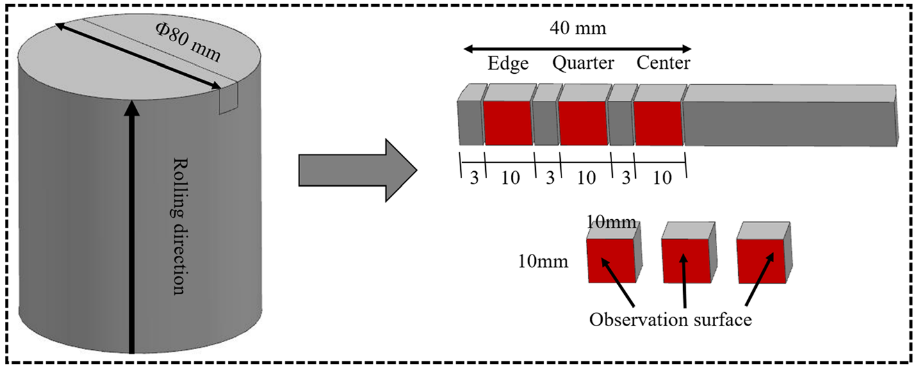

Fig. 1 Schematic diagram of rolled steel treatment

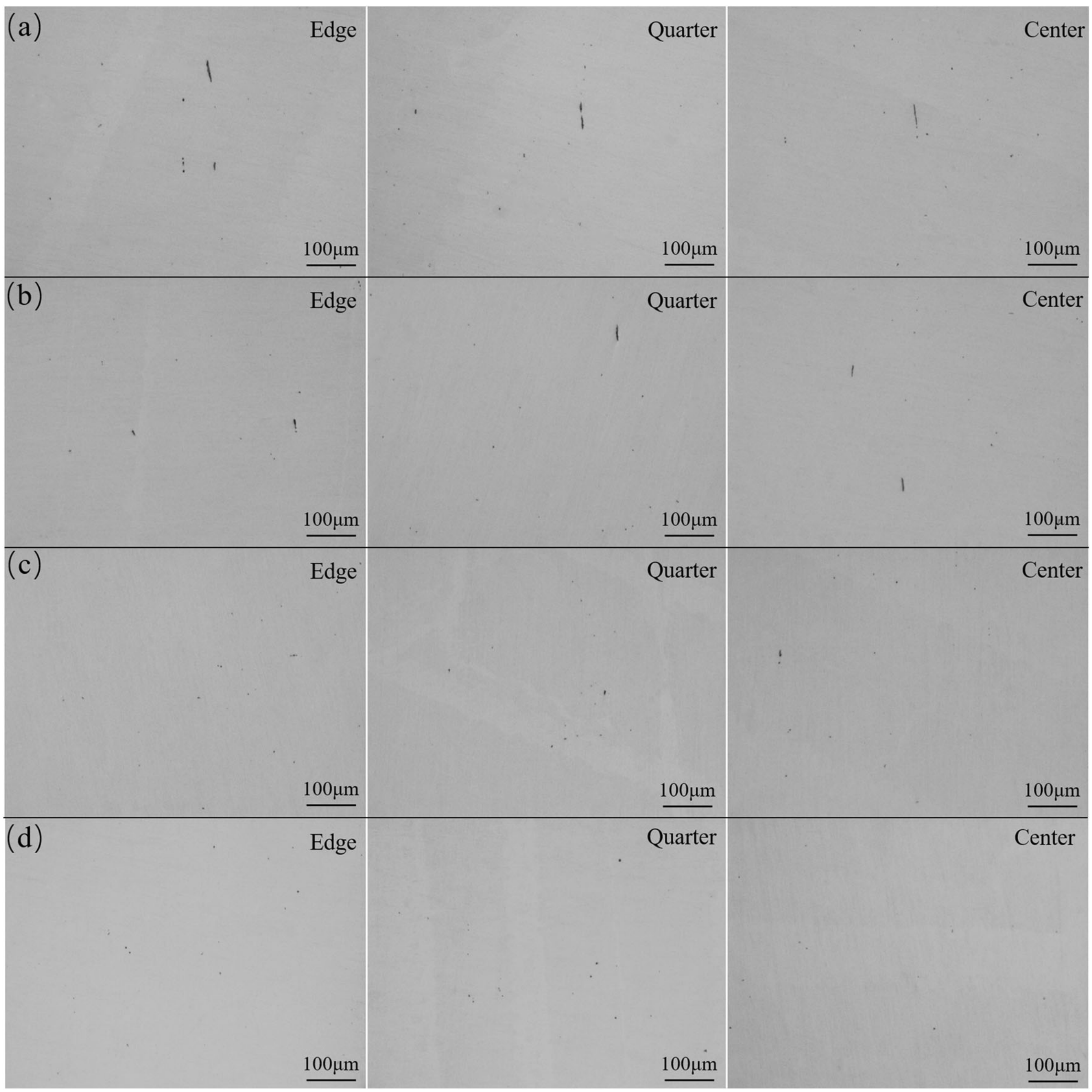

Fig. 2 Optical morphology and distribution of inclusions at various positions in rolled steel of GCr15 bearing steel with different La-Ce additions: **a** 0 ppm, **b** 50 ppm, **c** 100 ppm, **d** 150 ppm

was uniform. Therefore, although La-Ce could not significantly reduce the number of inclusions, it promoted the uniform distribution of inclusions, consistent with the results observed in Fig. 2.

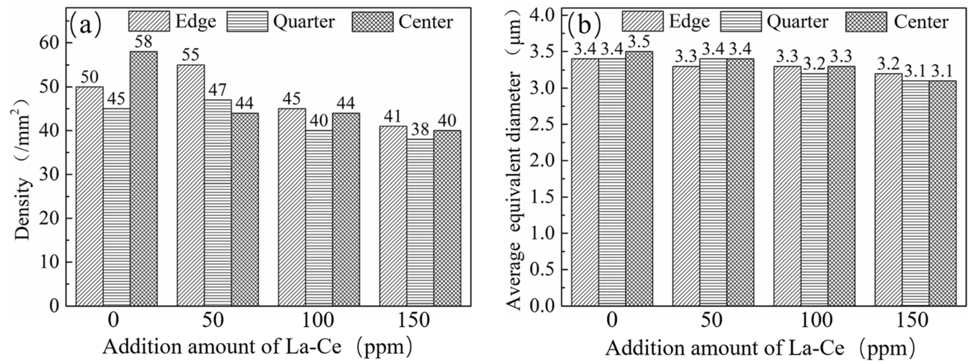

Fig. 3 Quantity and size of inclusions at various positions in rolled steel of GCr15 bearing steel with different La-Ce addition: **a** density, **b** average equivalent diameter

Figure 3b shows that La-Ce had little effect on the average size of inclusions. When La-Ce was not added, the average equivalent diameter of inclusions was 3.4 μm, while it decreased to 3.1 μm with increase in the addition, inconsistent with the phenomenon that long strip inclusions decreased remarkably with the addition of La-Ce observed in Fig. 2. So to deeply analyze the effect of La-Ce on inclusion size, the aspect ratio of inclusions and the proportion of inclusions with different sizes were counted and calculated, as shown in Fig. 4.

Figure 4a shows that when La-Ce was not added, the proportion of inclusions with aspect ratio of more than 3 in the steel was about 26%; with increasing addition, the proportion began to decrease; as the addition reached 150 ppm, the proportion decreased to 10%. A similar conclusion can be drawn in Fig. 4b. With the increase in La-Ce addition, the proportion of inclusions with sizes more than 10 μm began to decrease. This indicated that La-Ce had limited effect on the entirety size of inclusions, but could remarkably refine large-size inclusions.

3.1.2 Effect of La-Ce on the Type and Morphology of Inclusions

There were three typical inclusions in GCr15 bearing steel, namely MnS, Al_2O_3 and their composite inclusions. The morphology and composition analyses of them in steel were determined by SEM + EDS as shown in Fig. 5. Due to the low hardness of MnS inclusions, they are easy to deform along the rolling direction, most of MnS inclusions in the rolled steel were spindle, and the rest showed slender strip shape with large aspect ratio. The slender long-strip MnS inclusions significantly affected the mechanical properties of the material [16]. Because the large amount of Al was added for deoxidation in the smelting process, the oxide inclusions in the steel were mainly Al_2O_3. Although Al_2O_3 inclusions have high hardness and are not easy to deform during rolling, their overall morphologies were poorly controlled. Furthermore, the crystal structure of Al_2O_3 is angular which has a strong destructive effect on the matrix, thus resulting in a certain impact on the strength of the material [17, 18].

When the addition of La-Ce reached 50 ppm, Al_2O_3 and $MnS{\cdot}Al_2O_3$ were transformed into $RE\text{-}S{\cdot}Al_2O_3$ (RE was La-Ce), $RE\text{-}S\text{-}Mn{\cdot}Al_2O_3$ and $RE\text{-}S\text{–}O\text{-}Al{\cdot}Al_2O_3$ rare earth inclusions, and their morphologies are shown in Fig. 6. EDS analyses indicate that the elements in the white area of inclusions were mainly S, La and Ce, and others also contained Al, O and Mn, indicating that La-Ce mainly experienced desulfurization to form RE-S inclusions, resulting in the reduction in the quantity and size of MnS.

As shown in Fig. 7, when the addition of La-Ce reached 100 ppm, most slender strip MnS inclusions in the rolled steel disappeared, and the white rare earth inclusions began

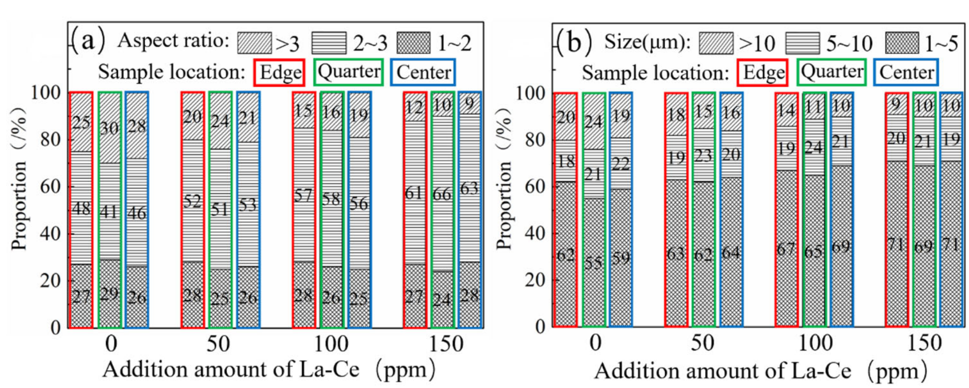

Fig. 4 Proportion of inclusions in rolled steel of GCr15 bearing steel with different La-Ce addition: **a** proportion of aspect ratio, **b** proportion of different sizes

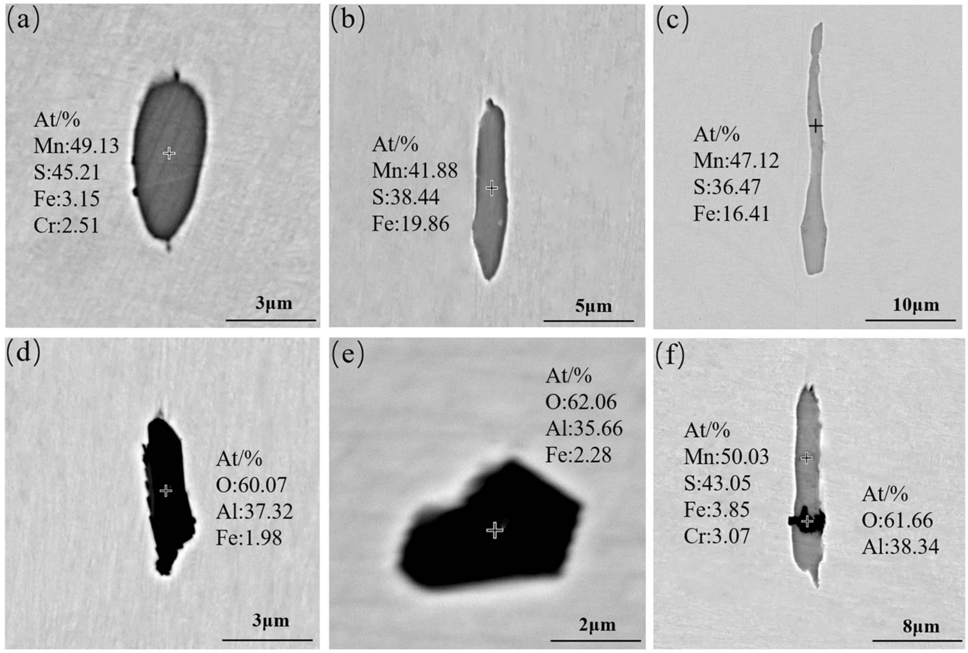

Fig. 5 SEM + EDS of typical inclusions in rolled GCr15 bearing steel without La-Ce addition

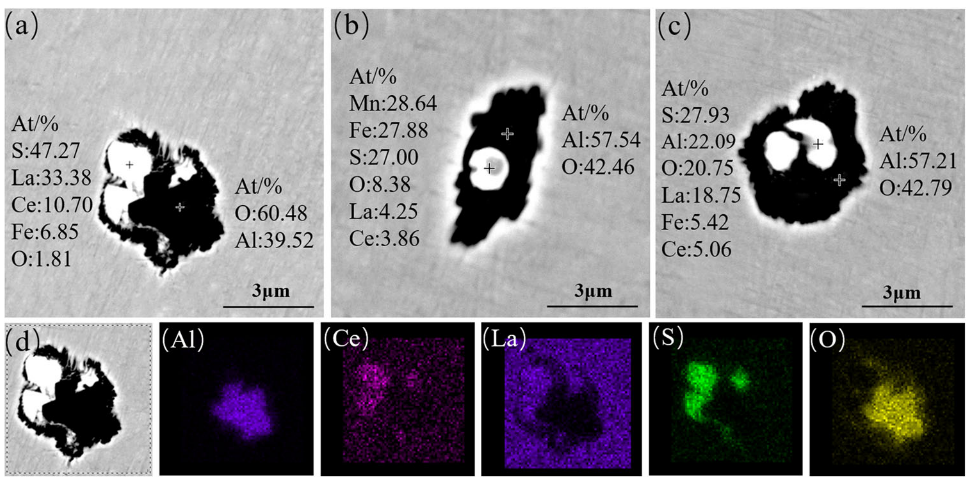

Fig. 6 SEM + EDS of rare earth inclusions in rolled GCr15 bearing steel with La-Ce addition of 50 ppm

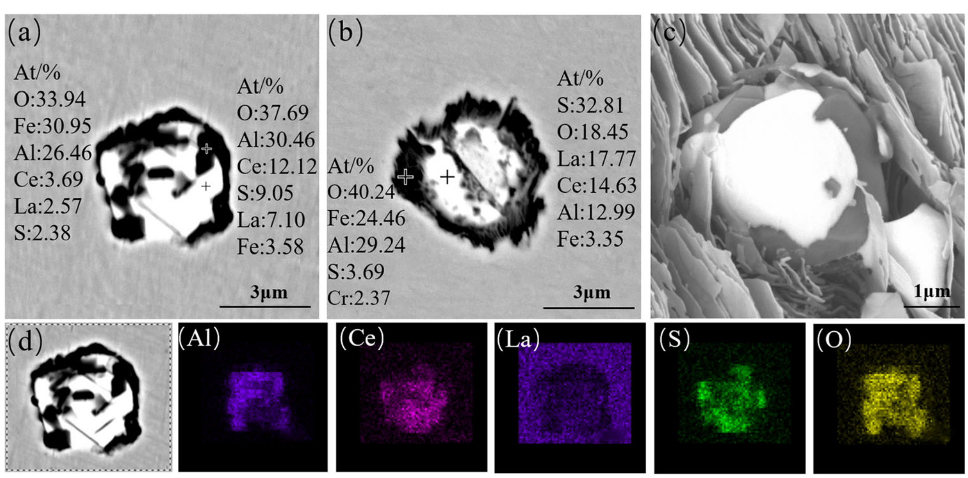

Fig. 7 SEM + EDS of rare earth inclusions in rolled GCr15 bearing steel with La-Ce addition of 100 ppm

to wrap Al_2O_3. Further EDS analysis shows that the type of white rare earth inclusions had changed from RE-S to RE–O-Al-S inclusions, indicating that La-Ce reacted with Al_2O_3. Figure 7c shows the 3D morphology of rare earth inclusion by electrolytic corrosion. After La-Ce modification, the original angular morphology of inclusions was changed to spherical shape, indicating that La-Ce had the function of spheroidizing inclusions.

When the addition of La-Ce was 150 ppm, the white rare earth inclusions had completely wrapped Al_2O_3. According to the EDS analysis, the Al content in the inclusions was at a very low level, indicating that Al_2O_3 basically disappeared and was completely modified into RE–O-S rare earth inclusions. As shown in Fig. 8, the overall morphology of inclusions was spherical.

3.2 Modification Mechanism of Inclusions in GCr15 Bearing Steel by La-Ce

3.2.1 Formation Law of Rare Earth Inclusions in GCr15 Bearing Steel

Through the above comprehensive analysis, it can be found that La-Ce could not only reduce the quantity and the size of MnS, but also promote the transformation of Al_2O_3 to spherical rare earth inclusions, and the overall modification effect improved with the increase in La-Ce addition. In order to deeply explore the modification mechanism of rare earth on inclusions, it is necessary to analyze the influence of Ce/La on inclusions, respectively.

In this industrial test, La-Ce rare earth alloy was added to liquid steel at 1610 ~ 1620 °C, and the liquidus temperature of GCr15 bearing steel was 1440 °C, calculated by the FactSage software. Therefore, to explore the modification mechanism of La-Ce rare earth on the inclusions under smelting temperature, the effects of different Ce and La contents on inclusions in GCr15 bearing steel at 1450 ~ 1650 °C were calculated thermodynamically. In addition, EDS analysis shows that there were many RE–O-S inclusions in the GCr15 bearing steel after adding rare earth, but the database lacks the thermodynamic data of Ce_2O_2S and La_2O_2S. Therefore, based on the provided thermodynamic data of Ce_2O_2S from the relevant literature [19], the additional data was added to the FactSage software database in this paper for calculation. Considering that the Gibbs free energy of La_2O_2S is very close to Ce_2O_2S [20], it was also added to the database as the thermodynamic data of La_2O_2S. The thermodynamic data are shown in Table 2, and the calculated results are shown in Fig. 9.

As shown in Fig. 9a, when Ce was added to the liquid steel, Al_2O_3 would be modified into $CeAlO_3$ as Eq. (1). As the Ce content exceeded 23 ppm, it would react with $CeAlO_3$ to form Ce_2O_3 as Eq. (2); when the Ce content exceeded 46 ppm, $CeAlO_3$ was completely modified. The whole process of Ce modifying Al_2O_3 was determined by the Ce content, less affected by temperature. However, when Ce began to react with S, this reaction was affected by both temperature and Ce content. With the addition of Ce, it would react with Ce_2O_3 and S to form Ce_2O_2S as Eq. (3). When the content of Ce reached 86 ppm, Ce would react directly with S to form CeS as Eq. (4). In addition, as shown in Fig. 6, when the addition of La-Ce was 50 ppm, RE-S inclusions already existed and were attached to the surface of Al_2O_3, which indicated that when the addition amount of Ce was low, CeS would precipitate on the surface of Al_2O_3 as the core during solidification.

$$[Ce]+(Al_2O_3)=(CeAlO_3)+[Al] \quad \Delta G\Theta=-141264-29.5\,T(J/mol) \tag{1}$$

$$[Ce]+(CeAlO_3)=(Ce_2O_3)+[Al] \quad \Delta G\Theta=-62300-4.8\,T(J/mol) \tag{2}$$

$$Ce+\frac{3}{2}[S]+(Ce_2O_3)=\frac{3}{2}(Ce_2O_2S) \quad \Delta G\Theta=-598340+137.2\,T(J/mol) \tag{3}$$

$$[Ce]+[S]=(CeS) \quad \Delta G\Theta=-422100+120.38\,T(J/mol) \tag{4}$$

Figure 9b shows similar results, and with increasing La content, the transformation law of inclusions was $Al_2O_3 \rightarrow LaAlO_3 \rightarrow La_2O_2S \rightarrow La_2O_2S + La_2S_3$. The modification effect of La on Al_2O_3 was very close to that of Ce. The binding ability of La and S is stronger than that

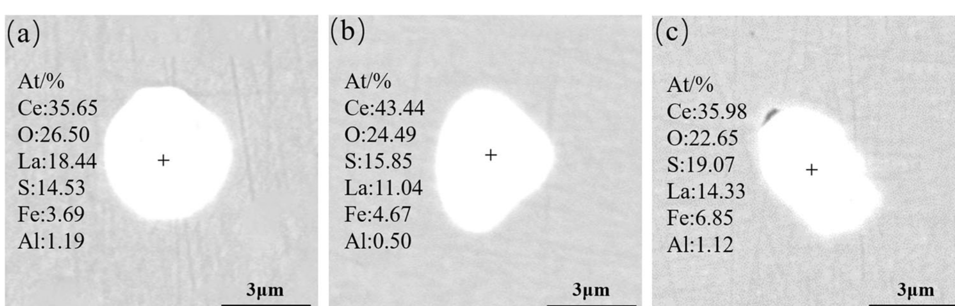

Fig. 8 SEM + EDS of rare earth inclusions in rolled GCr15 bearing steel with La-Ce addition of 150 ppm

Table 2 Thermodynamic data of Ce_2O_2S [19]

Compound	ΔH_{298}/(J mol^{-1})	ΔS_{298}/(J mol^{-1}·K^{-1})
Ce_2O_2S	− 1,696,600	130.5

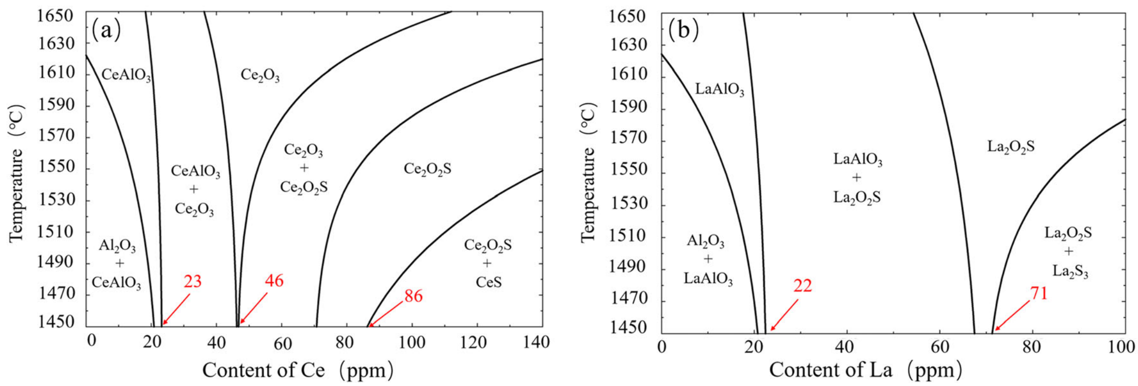

Fig. 9 Variation of inclusions in GCr15 bearing steel with Ce/La content with temperature: **a** Ce, **b** La

of Ce and S, so $LaAlO_3$ would directly react with S and La to form La_2O_2S. Moreover, the thermodynamic conditions required for the formation of La_2S_3 were lower than CeS. Therefore, although the mass ratio of La and Ce in the rare earth alloy used in this industrial test was 1:2, the content of La in RE-S inclusions was still significantly higher than Ce as shown in Fig. 6.

3.2.2 Modification Efects of Different La-Ce Contents on Inclusions

Through the above analysis, the transformation laws of rare earth inclusions were determined. Next, the specific addition of rare earth and its modification effect needed to be analyzed. In this test, La-Ce mixed rare earth was added to liquid steel for desulfurization and spheroidizing inclusions, so it is necessary to study the addition amount of La-Ce from these two aspects.

From the viewpoint of desulfurization, the reactions of La-Ce with S occurring in liquid steel are strongly expected before RH refining to form rare earth sulfides, partially removed during RH refining to reduce S content in liquid steel and to improve the morphology and quantity of MnS inclusions. From the viewpoint of spheroidizing inclusions, the reactions of La-Ce with Al_2O_3 occurring in liquid steel were strongly expected before solidification of liquid steel to form the rare earth inclusions in spherical shape. Therefore, the effects of different La-Ce contents on inclusions in GCr15 bearing steel at 1600 and 1450 °C were calculated by FactSage software, as shown in Fig. 10.

The addition amount of La-Ce in furnace B, C and D in the tests was 50, 100 and 150 ppm, respectively. According to previous production experience, the overall yield of rare earth added to liquid steel at the end of LF refining without RH treatment is 20 $\sim$ 30%. Based on the average yield of 25%, the contents of La and Ce in furnaces B, C and D before RH refining were 4 and 8 ppm, 8 and 16 ppm, 16 and 24 ppm, respectively. As shown in Fig. 10a, at 1600 °C, RE–O-S existed only in furnace D, so the content of S in this furnace was lowest. Although there was no RE–O-S in furnace C, the La-Ce content was near the critical value for the formation of it. Therefore, with decreasing temperature, RE–O-S would be formed and absorbed by covering agent in the tundish refining process. Although the removal effect was limited, it would also reduce the content of S in steel, which was consistent with the overall changed trend of S content shown in Table 1.

Figure 10b shows that the inclusions in furnace B were $REAlO_3$ and Al_2O_3, so the overall morphology of inclusions in Fig. 6 was still in irregular shape. In furnace C, the morphology of inclusions had been significantly improved because Al_2O_3 had been completely modified, while in furnace D, $REAlO_3$ had been further modified to RE_2O_3 in spherical shape, as shown in Fig. 8.

Through the comprehensive analysis of Fig. 10, it could be seen that under La-Ce mass ratio of 1:2 and their contents at least 7.5 and 15 ppm, Al_2O_3 could be completely modified in the GC15 bearing steel; when reaching at least 10 and 20 ppm, the S content in steel was effectively reduced to significantly improve the morphology and quantity of MnS inclusions.

By adding additional thermodynamic data to FactSage software, the phase diagrams of the effect of La-Ce content on inclusions under different temperatures were obtained,

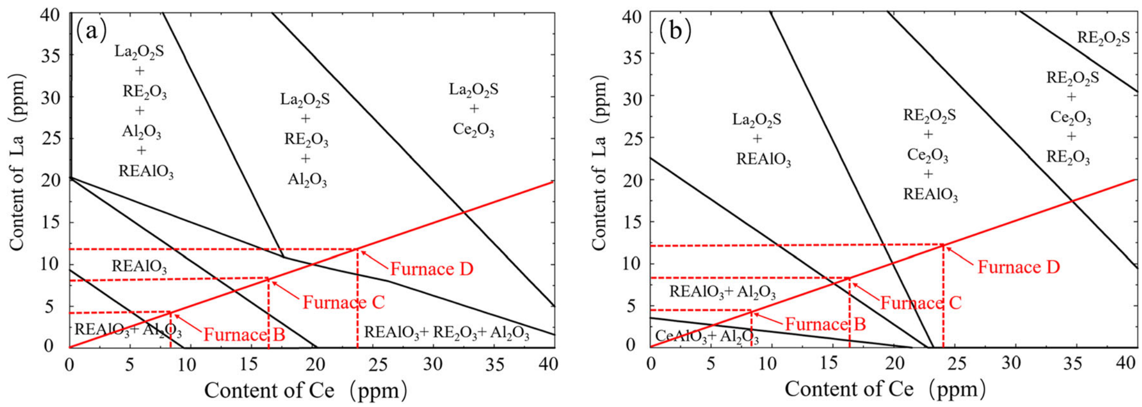

Fig. 10 Effect of La-Ce content on inclusions at different temperatures: **a** 1600 °C; **b** 1450 °C

which were very consistent with the actual transformation of inclusions. In subsequent industrial production, this phase diagram could be used to determine the optimal addition amount of La-Ce.

Therefore, considering the production cost and modification effect, when the addition amount of La-Ce reached 90 ppm or more, the overall morphology of inclusions effectively improved, and the S content in the steel got significantly reduced when the addition amount reached 120 ppm in the industrial production of La-Ce modifying GCr15 bearing steel in the future.

4 Conclusions

This work aimed to study the modification effect and its mechanism of La-Ce addition on the inclusions in GCr15 bearing steel. The following conclusions are obtained.

(1) The typical inclusions in GCr15 bearing steel were long strip MnS and irregular Al_2O_3. The addition of La-Ce reduced the quantity and size of inclusions and improved their overall morphologies.

(2) With increasing La-Ce content, the transformation sequence of inclusions in GCr15 bearing steel was $Al_2O_3 \rightarrow REAlO_3 \rightarrow RE_2O_3 \rightarrow RE_2O_2S \rightarrow RE_2O_2S + RE_xS_y$, but with decreasing temperature, RE_xS_y would also precipitate during solidification when the La-Ce content was low.

(3) The RE_2O_2S and RE_xS_y formed by La-Ce desulfurization reduced the quantity and size of MnS. The morphologies of $REAlO_3$ and RE_2O_3 formed by La-Ce replacing Al were closer to spherical shape than Al_2O_3.

(4) The phase diagram analysis shows that in the industrial test, the morphology of inclusions in GCr15 bearing steel could be significantly improved when the addition amount of La-Ce reached 90 ppm; when the addition amount reached 120 ppm, the S content could be significantly reduced.

References

1. Zhong YB, Fang YP, Peng MH et al. (2016) Effect of transverse static magnetic field on microstructure and properties of GCr15 bearing steel in electroslag continuous casting process. Materials Science & Engineering, A **660**: 118-126.
2. Lu L, Li W, Zhang J et al. (2009) Analysis of rotary bending gigacycle fatigue properties of bearing steel GCr15. Acta Metallurgica Sinica **45(1)**: 73-78.
3. Hashimoto K, Fujimatsu T, Tsunekage N et al. (2011) Study of rolling contact fatigue of bearing steels in relation to various oxide inclusions. Materials & Design **32(3)**: 1605-1611.
4. Nmark N, Karasev A, Nsson P. (2015) The effect of different non-metallic inclusions on the machinability of steels. Materials **8(2):** 751-783.
5. Mayer H, Haydn W, Schuller R, et al. (2009) Very high cycle fatigue properties of bainitic high carbon-chromium steel. International Journal of Fatigue **31(2)**: 242-249.
6. Guan J, Wang LQ, Zhang CW, et al. (2017) Effects of non-metallic inclusions on the crack propagation in bearing steel. Tribology International **106**: 123-131.
7. Xie JB, Zhang D, Yang QK, et al. (2019) Exploration of morphology evolution of the inclusions in Mg-treated 16MnCrS5 steel. Ironmaking & Steelmaking **46(6)**: 564-573.
8. Yang SF, Li JS, Wang ZF, et al. (2011) Modification of MgO·Al_2O_3 spinel inclusions in Al-killed steel by Ca-treatment. International Journal of Minerals, Metallurgy and Materials **18(1)**: 18-23.
9. Pan F, Jian Z, Chen H L et al. (2016) Thermodynamic calculation among cerium, oxygen, and sulfur in liquid iron. Scientific Reports **6(1)**: 1-6.
10. Wang H, Li X, Zhang L et al. (2017) Investigation of RE-O-S-As inclusions in high carbon steels. Metallurgical & Materials Transactions B **48(6)**: 2849-2858.
11. Bohlen J, Yi S, Letzig D, et al. (2010) Effect of rare earth elements on the microstructure and texture development in magnesium-manganese alloys during extrusion. Materials Science & Engineering A **527(26)**:7092-7098.
12. Xin WB, Song B, Song MM, et al. (2015) Effect of cerium on characteristic of inclusions and grain boundary segregation of

arsenic in iron melts. Steel Research International **86(12)**: 1430-1438.
13. Li H, Yu YC, Ren X, et al. (2017) Evolution of Al_2O_3 inclusions by cerium treatment in low carbon high manganese steel. Journal of Iron and Steel Research, International **24(9)**: 925-934.
14. Gong W, Wang C, Wang PF, et al. (2021) Effect of La on inclusions and fracture toughness of low-alloy ultra-high-strength 40CrNi2Si2MoVA steel. Journal of Iron and Steel Research International **28**:1408-1416.
15. Ren Q, Zhang LF. (2020) Effect of Cerium Content on Inclusions in an Ultra-Low-Carbon Aluminum-Killed Steel. Metallurgical and Materials Transactions B **51(2)**: 589-600.
16. Kawakami K, Tsuyoshi T, Kunihiko N (2007) Generation mechanisms of non-metallic inclusions in high-cleanliness steel. Tetsu-to-Hagane **93(12)**: 743-752.
17. Yang CY, Luan YK, Li DZ, et al. (2018) Very high cycle fatigue properties of bearing steel with different aluminum and sulfur contents. International Journal of Fatigue **116**: 396-408.
18. Spriestersbach D, Grad P, Kerscher E. (2014) Influence of different non-metallic inclusion types on the crack initiation in high-strength steels in the VHCF regime. International Journal of Fatigue **64**: 114-120.
19. Knacke O, Kubaschewski O, Hesselmann K. (1992) Thermochemical properties of inorganic substances. Berlin: Springer-Verlag.
20. Geng R, Li J, Shi CB, et al. (2020) Effect of Ce-La on inclusion evolution in Al-killed high strength steel. Metallurgical Research and Technology **117(6)**: 616-623.

Publisher's Note Springer Nature remains neutral with regard to jurisdictional claims in published maps and institutional affiliations.